Computer-controlled Raman spectrometer for time-resolved measurements in low-pressure gaseous samples

Eric Mazur

Department of Physics and Division of Applied Sciences, Harvard University, Cambridge, Massachusetts 02138

(Received 10 March 1986; accepted for publication 30 June 1986)

A spectrometer for measuring spontaneous Raman scattering in gaseous samples at pressures below 100 Pa (0.75 Torr) with nanosecond time resolution is presented. The apparatus was developed for studying intramolecular vibrational energy distributions in infrared multiphoton excited molecules and makes it possible to study the anti-Stokes Raman scattering from isolated molecules at pressures down to 14 Pa (110 mTorr). To achieve high sensitivity and time resolution simultaneously, spectral resolution (1 nm) is sacrificed. Because of the low level of the signals, the measurements are completely computer controlled. A detailed description of the apparatus, including the multichannel data-acquisition hardware and computer interface, is given.

INTRODUCTION

Since the cross sections for spontaneous Raman transitions are extremely small,[1] experiments on spontaneous Raman scattering are normally performed at high pressure. There are circumstances, however, under which a high pressure is not desirable. One example is the study of collisionless infrared multiphoton excitation.[2] Since the aim of this study is to observe vibrational energy distributions in *isolated* molecules, the observation time has to be several orders of magnitude smaller than the average time between molecular collisions, which puts an upper limit on the sample pressure. For times of the order of magnitude of nanoseconds this means a pressure below 100 Pa (0.75 Torr), at least three orders of magnitude lower than usual for Raman spectroscopy.

This paper presents the details of an apparatus that has allowed measurements of spontaneous Raman scattering on a nanosecond time scale at pressures down to 14 Pa, i.e., from virtually isolated molecules. The apparatus has a large collection efficiency and effectively reduces stray light, which forms the major obstacle when measuring Raman scattering at low pressures. Because the signals are in the photon counting regime and extensive averaging is required, the measurements are completely automated.

Apart from the detection method presented here, there are several other possibilities for measuring Raman scattering from isolated molecules. For example, one can use a molecular beam or jet,[3] or one can resort to more sensitive spectroscopy techniques, such as coherent anti-Stokes Raman spectroscopy.[4] Both methods, however, require additional equipment and may have certain disadvantages. The first method requires a molecular beam apparatus and extensive vacuum equipment. Moreover, measurements are carried out in a nonequilibrium situation. Coherent anti-Stokes Raman spectroscopy, on the other hand, requires a much more elaborate laser setup, but has a higher sensitivity and higher spectral resolution. Moreover, at very low densities spontaneous Raman scattering is more efficient than coherent anti-Stokes Raman spectroscopy, which is proportional to the density squared. For certain research projects, such as the one discussed here, the research goal can be accomplished with a careful design of the scattering cell, and a convenient and flexible multichannel data-acquisition system.

The design of the scattering cell may also be useful in other light scattering experiments that require maximum collection efficiency and minimum stray light. A detailed description of the setup is given below, and representative experimental results obtained with the apparatus are presented.

I. GENERAL LAYOUT

The design of the scattering cell is based on the following experimental approach. A sample of low-pressure gas (typically 100 Pa or lower) is excited by an infrared pulse from a high-power picosecond CO_2 laser (100 mJ in 500 ps or less). After a short controlled time delay the excited molecules are probed by an ultraviolet pulse (30 mJ in 18 ns) from a frequency-doubled ruby laser.

For a strong Stokes Raman transition at a sample pressure of 100 Pa, one can expect a Raman signal of about 20 photons/sr per mJ input power of the probing pulse. For a fixed pressure the signal can only be increased by either increasing the collection angle or the input power. At the same time one has to minimize the effect of unwanted, elastically scattered light. The two main contributions to elastically scattered light are Rayleigh scattering and stray light scattered from the windows and walls of the cell. Typically, the Rayleigh scattering is about four orders of magnitude more intense than the Stokes Raman signal. Stray light, which is independent of sample pressure, quickly becomes the dominant source of scattered light at low pressures. A scattering of only one in 10^9 photons into the detection angle already results in 1.6×10^6 photons/sr, per mJ of input power. Therefore, to be able to measure Raman scattering at low pressures, one has to optimize collection efficiency and mini-

 0034-6748/86/102507-05$01.30

mize stray light in the design of the scattering cell on one hand, and simultaneously maximize the rejection of unwanted signal in the detection.

A. Scattering cell

The cell, in which the exciting and probing laser beams cross at right angles, is shown in Figs. 1 and 2. It consists of a cube-shaped aluminum body with two pairs of arms of circular cross section. The arms for the exciting infrared beam are 0.15 m long, the ones for the probing ultraviolet beam 0.3 m. In order to minimize stray light from the windows the long arms have quartz windows at Brewster angle. In addition, each of these arms contains six pairs of straight [see Fig. 2(a), D1] and conical (D2) baffles. The straight baffles collimate and restrict the probe beam, while the conical baffles trap any light scattered along the path of the beam.[5] The baffles are made separately from the arms and are installed by sliding them into the arms, so that they can be arranged in various configurations. The best results were obtained with apertures increasing from 2 mm nearest to the windows to 4 mm nearest to the center of the cell. In the center part of the cell a vertical stray-light jacket (J) of circular cross section prevents any light scattered from the last baffle from reaching the detection aperture directly. It has two 6-mm holes for the probe beam and two 15-mm holes for the infrared beam. Light scattered at the intersection of the two beams is collected over a solid angle of $\pi/16$ sr and collimated by a quartz lens (L) that serves as a window. The focus of this lens coincides with the intersection of the two beams. All parts of the cell are vapor blasted and black anodized to absorb as much stray light as possible. A gas inlet on the bottom plate connects the cell to a gas-handling and vacuum system.

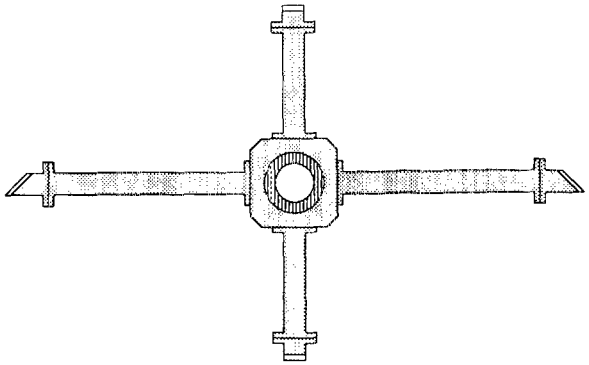

FIG. 1. Top view of the low-pressure Raman cell. The CO_2-laser beam (pump) enters through the short arms, while the probing UV beam enters through the long arms. Scattered light exits through a collimating lens at the top.

To simplify the alignment of the laser beams, the cell is mounted on four tightly fitting posts (P) shown in Fig. 2(b). It can easily be removed and put back accurately by lifting a black nylon shaft (S) through which the collimated scattered light reaches the detection. Alignment of the beams is achieved as follows. First, a He-Ne laser beam is aligned through the probe arms. Then the cell is removed and two diaphragms are centered on the beam, one in front of and one behind the cell. Finally, the pulsed probe beam is aligned through the two diaphragms and subsequently optimized through the cell. To overlap the two beams, the cell is again removed after the alignment of the probe beam, and the infrared beam is adjusted until the two beams produce overlapping burn spots on a piece of thermo-fax infrared copy paper. Final adjustments are made by optimizing the signal.

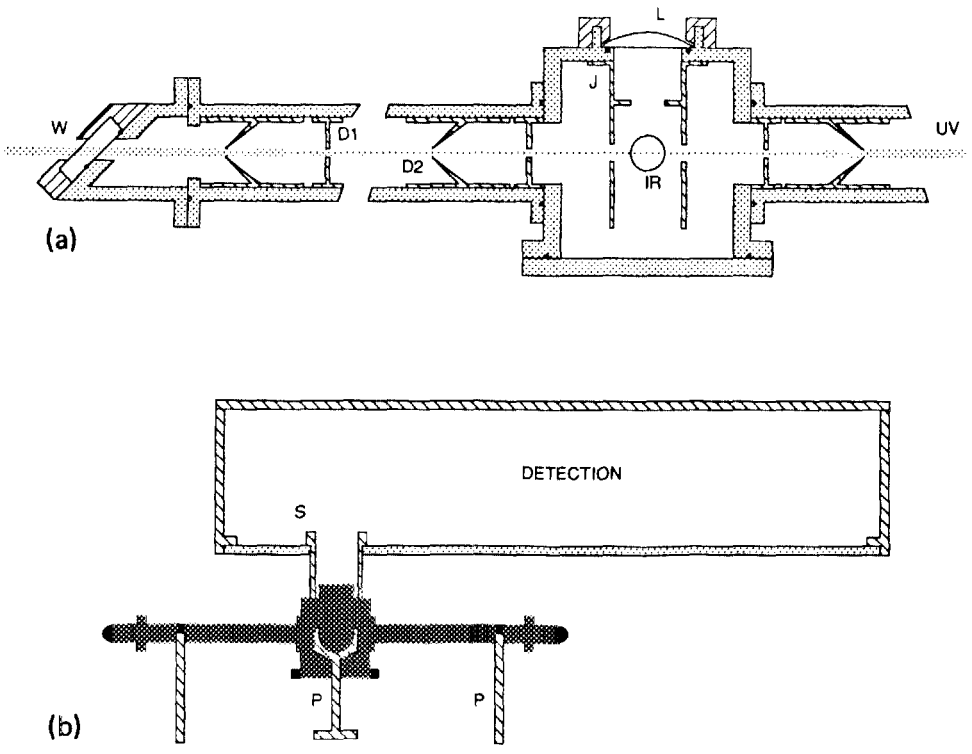

FIG. 2. Cross-sectional (a) and side view (b) of the Raman cell. W = quartz window, D1, D2 = straight and conical baffles, J = stray light jacket, IR = position of IR pump beam, UV = probing UV beam, L = collimating lens. The cell is mounted on four posts, P, from which it can easily be removed by lifting the light shaft, S, through which the scattered light reaches the detection hardware. The window holder in the upper drawing has been rotated by 90° to show the Brewster angle mounting.

B. Detection

The scattered light is analyzed in a light-tight enclosure on a raised platform above the scattering cell [see Figs. 2(b) and 3]. The scattered light that exits the cell consists of Stokes and anti-Stokes Raman signals, Rayleigh scattering, and stray light. A dichroic mirror and a quartz lens image the scattering region onto the entrance slit of a double monochromator. The imaging ratio of the detection lenses is 2 : 1, so that the 6×2-mm entrance slit of the monochromator corresponds to a 3×1 mm area of the scattering region. Additional spatial filtering between the two monochromators further reduces stray light. Since high spectral resolution is not a requirement for the present study, two small 0.25 m $f/3.5$ monochromators were employed. Apart from their high throughput, small monochromators have a high rejection ratio (typically 10^9), which is needed to eliminate the elastically scattered light. The total throughput of the two monochromators is about 4%. A photomultiplier is mounted directly onto the exit slit of the monochromator in a thermoelectrically cooled housing.

C. Specifications

The overall signal-to-noise ratio of cell and detection is excellent: Even though single photons are registered for each laser pulse, the measurements can be performed in daylight or with room lights on. The amount of ambient light that reaches the photomultiplier after the spatial and spectral filtering is well below the 1.5-kHz dark count rate of the photomultiplier tube and therefore entirely negligible. The amount of stray light detected just behind the entrance slit of the monochromator after evacuating the cell is less than 10^{-10} of the probe beam and around 10^{-6} at the position of the lens. The overall detection efficiency, including the quantum efficiency of the photomultiplier is 3×10^{-4}.

II. HARDWARE DESCRIPTION

The general layout of the setup for measuring the Raman scattering from infrared multiphoton excitation is shown in Fig. 3. A description of the high-power picosecond CO_2-laser facility can be found in Ref. 6. The infrared pulse power is monitored by a pyroelectric detector (P2) and focused into the cell with a cylindrical ZnSe lens. The full width at half-maximum (FWHM) beam size at the intersection of the two laser beams is 0.35×6 mm. The output of the Q-switched ruby laser (300 mJ in 20 ns) is monitored by a fast silicon photodiode (FND) and frequency doubled with a temperature tuned RDA crystal. The resulting ultraviolet radiation at 347 nm is split off with a harmonic beam splitter, its polarization rotated in the plane of the two laser beams with a half-wave plate, and focused into the cell. The FWHM beam waist at the focus is 180 μm. The power of the ultraviolet pulse (30 mJ in 18 ns) is monitored with a Hamamatsu phototube. The scattered light is focused onto the entrance slit of a tandem Jarrel-Ash 0.25-m Ebert-type monochromator with 2400 grooves/mm gratings. The linear dispersion of the system is 1.65 nm/mm. Most measurements were carried out at a resolution of 3 nm, enough to prevent elastically scattered light from reaching the detector. The output of the monochromator is detected with a Amperex XP2020Q photomultiplier tube (1-ns time resolution, 1.5-kHz dark count rate, 25% quantum efficiency). A mechanical shutter (S) protects the tube when the detection box is opened.

Since the power of the CO_2 laser and the time delay between the two laser pulses are fluctuating considerably, and since the observed signals are in the photon counting regime, many thousands of laser shots (typically 10^4) are needed for a single experimental run. The data are sorted out after measurement, and the random fluctuations in power (and to a certain degree those in timing) provide the variation needed to obtain results as a function of these param-

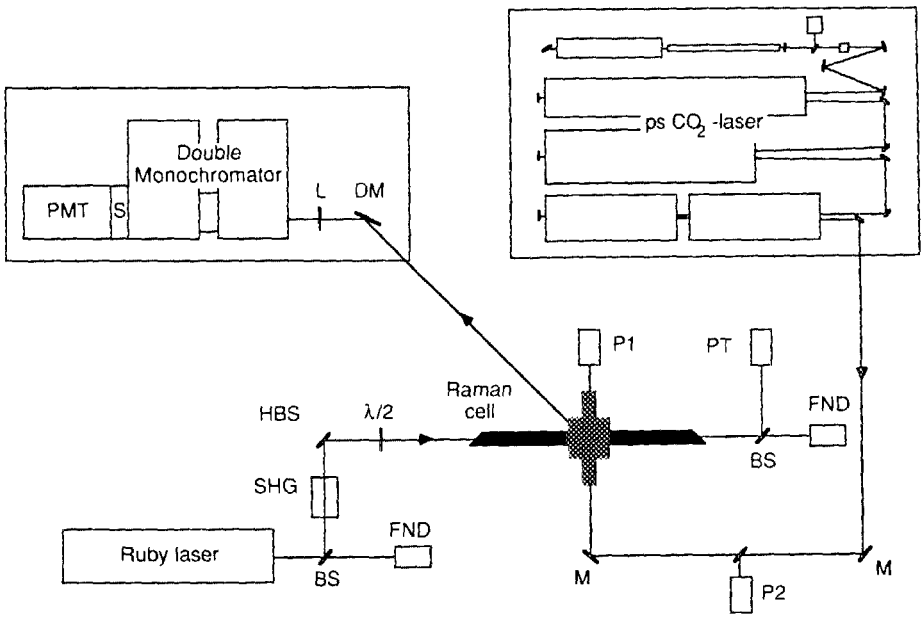

FIG. 3. Setup for measuring the spontaneous Raman scattering from infrared multiphoton excited molecules at low densities. Molecules excited by a CO_2 laser are probed by the second harmonic of a Ruby laser. BS = beam splitter, SHG = second-harmonic generator, HBS = harmonic beam splitter, $\lambda/2$ = half-wave plate, FND = fast photodiode, PT = phototube, P1, P2 = pyroelectric detector, M = mirror, DM = dichroic mirror, L = quartz lens, S = shutter, and PMT = photomultiplier tube. The detection (monochromator, photomultiplier, etc.) is located in a light-tight enclosure located directly above the Raman cell. Drawing not to scale.

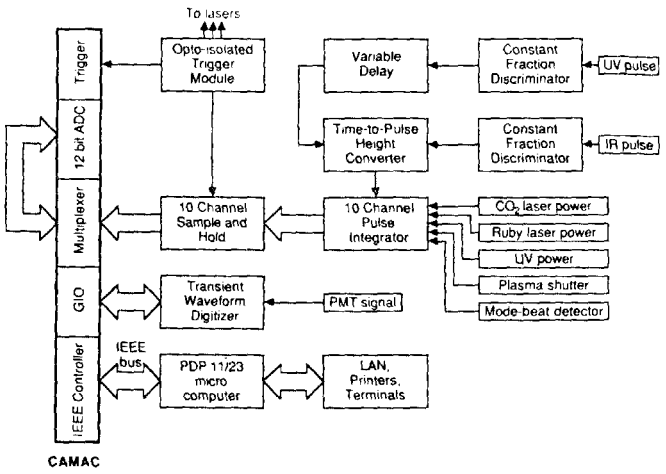

FIG. 4. Schematic view of the data-acquisition electronics.

eters. The long duration of the measurements and the large amount of data collected made it necessary to automate the data acquisition. Figure 4 shows a diagram of the data-acquisition electronics. The CO_2 laser is located in a rf shielded room to prevent interference with the data-acquisition electronics. Furthermore, all trigger connections with the two lasers are opto-isolated to prevent any feedback of noise via the trigger cables. The electronics are mounted in NIM (nuclear instrumentation module) racks and a CAMAC (computer automated measurement and control) crate.

A home-built master trigger module provides the trigger pulses for the ruby laser, Q switch, CO_2-laser and laser amplifiers, and the data acquisition. Even though the trigger pulses can be set with nanosecond accuracy, the inherent jitter of the lasers prevents synchronization better than 100 ns. Therefore, the time delay between pump and probe is measured for each pair of laser pulses. A fast pyroelectric detector (Fig. 3, P1) and a fast photodiode (FND), both with subnanosecond resolution, provide the start and stop pulses for an EG&G Ortec model 457 time to pulse-height converter. A variable delay for the start pulse allows both negative and positive time delays between the two pulses to be registered. To make the timing measurement independent of the fluctuations in intensity, the two pulses are first processed by an EG&G Ortec model 934 constant fraction discriminator. The overall accuracy of the time-delay measurement is better than 1-ns. The overall time resolution of the measurements, however, is limited by the 18-ns duration of the probe pulse.

The incoming data pulses (see Fig. 4) are integrated and sampled twice in each data-acquisition cycle, once 160 ms before and once immediately after the lasers fire. Thus one can correct for possible base-line drift during long measurements. A Kinetic Systems model 3531 multiplexer sequentially scans the incoming pulses to a Kinetic Systems model 3553-Z1C 12-bit analog-to-digital converter. The output from the photomultiplier tube is recorded by a Gould Biomation 8100 transient waveform digitizer and then read out to the CAMAC crate with a Standard Engineering model GIO-816 input/output register and interface. All data, i.e., the base-line data and signals from the integrators and the digitized waveform, are transferred to a microcomputer by a Kinetic Systems model 3988-G2A GPIB CAMAC crate controller. The computer analyzes the output from the photomultiplier tube, corrects for the tail of darkcounts that occurred just before the probe pulse, displays the resulting data, and stores them on a Winchester disk. Data analysis and display can be done on line at any point during the measurement. The computer is connected to a local area network of computing facilities for backups and further data handling.

The software is all written in C language. Up to 19 different channels can be measured and analyzed. The measurement program also allows manual input on one data channel. This is particularly useful when a signal needs to be measured as a function of a parameter that cannot be controlled or measured directly by computer, e.g., the alignment of certain optics, the optimization of the timing of the laser amplifiers, or calibrations. This feature has proven to be of great help during the development of the setup, and effectively means that *any* measurement, even in the photon counting regime, can be carried out with the same data-acquisition and analysis software.

The analysis programs allow the display of any combination of the datachannels on two axes. The data can also be calibrated, transformed, and averaged. Finally, theoretical curves can be fitted to the points obtained.

III. EXPERIMENTAL RESULTS

The apparatus is used to study the intramolecular vibrational distribution of energy in various infrared multiphoton excited molecules.[7] The scope of this research project is to determine whether the intramolecular vibrational energy distribution after multiphoton excitation corresponds to a common equilibrium among the various vibrational degrees of freedom of the molecules. This can be determined by measuring the intensity of different Raman lines.

Figure 5 shows the Stokes and anti-Stokes signals from the ν_1 mode of SF_6 as a function of the time delay between the pump (tuned to the ν_3 mode of SF_6) and probe pulses. A clear increase in the signals can be seen immediately after the multiphoton excitation at $t = 0$. This measurement was car-

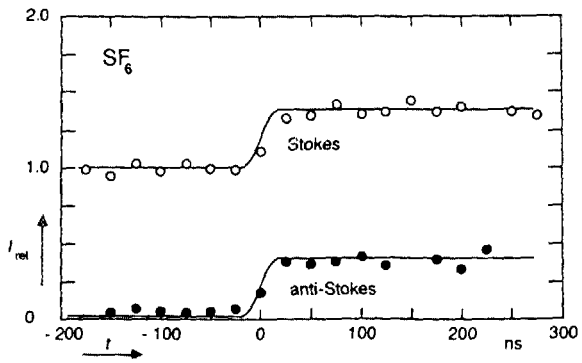

FIG. 5. Intensity of Stokes and anti-Stokes signals for SF_6 at a pressure of 133 Pa as a function of the time delay between pump and probe pulses. A negative delay means that the molecules are probed before they are excited. The signals are normalized to the thermal Stokes signals. The rise time in the curves reflects the 18-ns FWHM duration of the probe pulse.

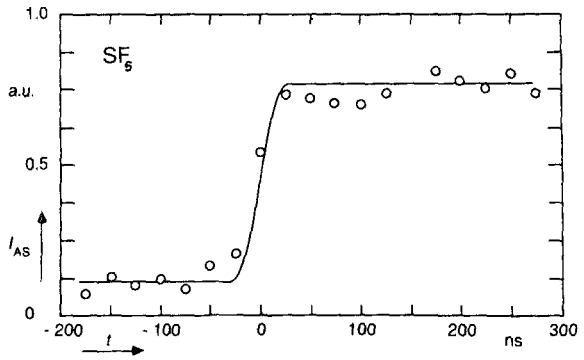

FIG. 6. Normalized intensity of the anti-Stokes signals for SF_6 at a pressure of 14 Pa as a function of the time delay between pump and probe pulses. The rise time in the curve reflects the 18-ns FWHM duration of the probe pulse.

ried out at a cell pressure of 140 Pa. The data were accumulated over a period of 10 h, or 6×10^3 laser pulses. Figure 6 shows that even at a pressure of 14 Pa good data can be obtained. The data in these two graphs have been averaged in 20-ns intervals. The same signal-to-noise ratio can be obtained with 5-ns intervals. It should be recalled, however, that in the present experimental setup the time resolution is limited by the 18-ns duration of the probe pulse. For full details of the measurements and a discussion of the results the reader is referred to Ref. 7.

Figure 7 shows two spectra obtained with the present apparatus at a cell pressure of 150 Pa. The spectral resolution, which is determined by the exit slit of the monochromator, is 3 nm. These graphs clearly show the capabilities of the

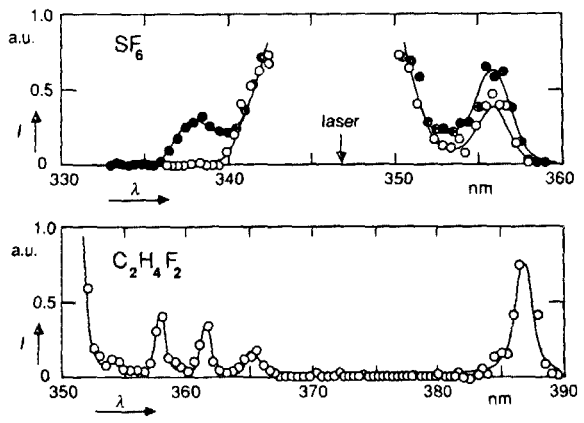

FIG. 7. Raman spectra for SF_6 (top) and $C_2H_4F_2$ (bottom) obtained at 150 Pa with (closed symbols) and without (open symbols) infrared excitation. The small vertical arrow shows the position of the probe pulse at 347.15 nm.

present setup and the feasibility of measuring spontaneous Raman scattering at these low pressures. There is no measurable contribution of stray light at the position of the Raman lines—at a shift of about 2 times the resolution of the spectrometer.

IV. DISCUSSION

The apparatus described above has been in use for well over a year now and has proven to be a valuable tool in the study of intramolecular dynamics. This apparatus has made it possible to carry out time-resolved spontaneous Raman spectroscopy in samples at pressures down to 14 Pa. The main features of the apparatus are the reduction of stray light, the high collection efficiency, the automated multichannel data acquisition, and integrated data handling, as well as proven reliability.

ACKNOWLEDGMENTS

I would like to thank Emil Sefner of the Gordon McKay Scientific Instrumentation Shop for his valuable advice in designing and building the Raman cell. This research was supported by the U.S. Army Research Office and the Joint Services Electronics Program under Contracts No. DAAG29-85-K-0600 and No. N00014-84-K-0465 with Harvard University.

[1] G. Herzberg, *Molecular Spectra and Molecular Structure* (van Nostrand, New York, 1950).

[2] See, e.g., W. Fuss and K. L. Kompa, Prog. Quantum Electron. 7, 117 (1981); D. S. King, in *Dynamics of the Excited State*, edited by K. P. Lawley (Wiley, New York, 1982); V. S. Lethokov, *Nonlinear Laser Chemistry*, Chemical Physics Series, Vol. 22 (Springer, Berlin, 1983); V. N. Bagratashvili, V. S. Lethokov, A. A. Makarov, and E. A. Ryabov, *Multiple Photon Infrared Laser Photophysics and Photochemistry* (Harwood, New York, 1984), and references therein.

[3] See, e.g., K. Bergmann, W. Demtröder, and P. Hering, Appl. Phys. 8, 65 (1975); D. H. Levy, L. Wharton, and R. E. Smalley, in *Chemical and Biochemical Applications of Lasers*, edited by C. Bradley Moore (Academic, New York, 1977).

[4] J. W. Nibler and G. V. Knighten, in *Raman Spectroscopy of Gases and Liquids*, edited by A. Weber (Springer, Berlin, 1979).

[5] The use of baffles is common practice in the design of scattering cells; see, e.g., K. D. van den Hout, P. W. Hermans, E. Mazur, and H. F. P. Knaap, Physica **104A**, 509 (1980); D. M. Brenner, J. Chem. Phys. **74**, 494 (1981).

[6] H. S. Kwok and E. Yablonovitch, Rev. Sci. Instrum. **46**, 814 (1975); J. G. Black, P. Kolodner, M. J. Schultz, E. Yablonovitch, and N. Bloembergen, Phys. Rev. A **19**, 704 (1979).

[7] E. Mazur, I. Burak, and N. Bloembergen, Chem. Phys. Lett. **105**, 258 (1984); Jyhpyng Wang, Kuei-Hsien Chen, and Eric Mazur, Phys. Rev. A (to be published).